CD73 alleviates GSDMD-mediated pyroptosis in spinal cord injury through PI3K/AKT/Foxo1 signaling

Shun Xu
Huashan Hospital Fudan University
Minghao Shao
Huashan Hospital Fudan University
Xiaosheng Ma
Huashan Hospital Fudan University
Jianyuan Jiang
Huashan Hospital Fudan University
Fan Zhang
Huashan Hospital Fudan University
Haocheng Xu
Huashan Hospital Fudan University
Wei Zhu
Huashan Hospital Fudan University
Feizhou Lu (lfzsubmission@163.com)
Huashan Hospital Fudan University https://orcid.org/0000-0001-8887-5554

Research

Keywords: CD73, GSDMD, Foxo1, Neuroinflammation, Pyroptosis, Spinal cord injury

Posted Date: February 20th, 2020

DOI: https://doi.org/10.21203/rs.2.18409/v2

Abstract

Background: Neuroinflammation-induced secondary injury is responsible for the sustained progression of spinal cord injury (SCI). Inflammatory programmed cell death or pyroptosis triggered by the pore-forming protein gasdermin D (GSDMD) is an essential step in neuroinflammation. The aim of this study was to determine the role of the immunosuppressive receptor CD73 in GSDMD-mediated pyroptosis following SCI.

Methods: CD73 deficient mice and LPS-stimulated BV2 cells were respectively used as the *in vivo* and *in vitro* models of microglial pyroptosis. Molecular and histological assays were performed to assess pyroptosis and inflammasome activation, and to explore the underlying mechanisms.

Results: CD73 inhibited the NLRP3 inflammasome and GSDMD, and decreased pyroptosis in the microglia via the adenosine-A_{2B} adenosine receptor (AR)-PI3K-AKT-FOXO1 pathway. Specifically, CD73 suppressed GSDMD at the transcriptional level through FOXO1. Furthermore, HIF-1α accumulation after SCI upregulated CD73, which in turn increased the expression of HIF-1α, resulting in a positive feedback regulatory loop.

Conclusion: CD73 alleviates microglial pyroptosis after SCI by inhibiting GSDMD via the adenosine-A_{2B}AR-PI3K-AKT-FOXO1 pathway.

Background

Spinal cord injury (SCI) is a debilitating condition that affects millions of people worldwide, and leads to severe motor defects in the regions below the injured segment [1]. Around 240,000-337,000 people are afflicted with SCI in the United States alone, and this number is estimated to grow by 17,000 annually [1]. Nearly 52% of these patients are paraplegic and 47% are quadriplegic [2]. The pathogenesis of SCI is complex and can be divided into two phases [3] – a transient initial traumatic phase, and a long-lasting secondary phase characterized by secretion of cytokines and chemokines at the lesion site and neurological damage [4]. Studies show that neuroinflammation plays a key role in the secondary phase of SCI [5],[6],[7].

Traumatic injury to the central nervous system (CNS) disrupts the blood spinal barrier, which triggers infiltration of immune cells and factors that cause axonal destruction, neuronal loss and demyelination. Studies have implicated cytoplasmic inflammasome complex in post-CNS trauma neuroinflammation [8], [9]. Inflammasomes are cytosolic multiprotein scaffolds assembled by specific pattern recognition receptors (PRRs), sensors of pathogen-associated molecular patterns (PAMPs) and damage-associated molecular patterns (DAMPs), and triggers the pro-inflammatory caspases [10]. Several inflammasome-associated sensors have been identified, including NLRP1, NLRP3, AIM2 and pyrin [11]. Inflammasomes formed by the assembly of these sensors, the scaffolding protein ASC and pro-inflammatory caspases

(caspase-1 and -4/5 in humans and caspase-1 and -11 in mice) autoactivate caspases and lead to the cleavage of proteolytic gasdermin D (GSDMD), resulting in pyroptosis [10].

Pyroptosis is an inflammatory form of programmed cell death wherein the activated cytosolic GSDMD [12] translocates to the plasma membrane, binds to the inner membrane lipids and oligomerizes to form membrane pores, resulting in local cell swelling, membrane rupture and extravasation of cytoplasmic DAMPs [13],[14],[15]. The latter recruit immune cells and aggravate the inflammatory cascade [16]. Microglia, the resident macrophages of the CNS, are the primary cellular mediators of innate immune responses [17] and pyroptosis [10],[18] following any injury. Pyroptosis mediated by microglia has in fact been implicated in the pathogenesis of multiple CNS diseases, including SCI and traumatic brain injury [19],[20], although the underlying mechanisms are unknown.

CD73, also known as ecto-5'-nucleotidase (NT5E), is an AMP hydrolase that breaks down extracellular ATP to adenosine [21]. It is a key regulator in various pathophysiological processes, and prevents excessive immune responses by maintaining the balance between pro-inflammatory ATP and immunosuppressive adenosine [22],[23]. Furthermore, CD73 exerts an anti-neuroinflammatory role in SCI by inhibiting macrophages/microglia polarization via the adenosine-p38 cascade [24]. Therefore, we hypothesized that CD73 attenuates inflammasome activation, inhibits microglial pyroptosis, and reduces neuroinflammation after SCI. To this end, we analyzed the levels of CD73 and GSDMD in the blood samples of SCI patients, and performed *in vitro* and *in vivo* functional assays to determine its role in microglial pyroptosis.

Methods

Donor recruitment and blood samples

Peripheral blood was collected from 20 SCI patients that presented at the Huashan Hospital, Fudan University from January 2019 to June 2019, and from 20 age- and sex-matched controls. The inclusion criteria for the patients were: (1) clear history of trauma and absence of any neurological abnormalities prior to SCI, (2) existing neurological abnormalities such as limb sensation, motor abnormality, and dysfunction of the bowel and bladder, and (3) MRI examination indicating spinal cord compression and altered neurotransmission. Patients undergoing methylprednisolone treatment, and those with a history of brain disease and spinal surgery were excluded. The severity of SCI was evaluated using the cervical dysfunction index (NDI) and American spinal injury association (ASIA) classification.

Quantitative real-time PCR (RT-PCR)

RNA was extracted from whole blood using GeneJET Stabilized and Fresh Whole Blood RNA Kit (ThermoFisher, CA, USA), and from the cells using TRIzol reagent (Invitrogen, San Diego, CA, USA) according to the manufacturers' instructions. RT-PCR was performed in the final reaction volume of 10μl using SYBR Green PCR Master Mix (ThermoFisher, CA, USA). GAPDH was used as the housekeeping gene and relative expression levels of the target mRNAs were calculated using the comparative ΔΔCT method.

Establishment of SCI model and treatment regimen

C57BL/6 CD73 knock out (KO) male mice were a gift from Prof. Thompson, Oklahoma Medical Research Foundation, Oklahoma City, USA. The wild-type (WT) male C57BL/6 mice were supplied by Shanghai SLAC Laboratory Animal Co., Ltd. (Shanghai, China). The mice used in this study are 8 weeks old. All animal experiments were approved by the Institutional Animal Care and Use Committee of Fudan University. As described in our previous study [24], the mice were anesthetized with intraperitoneal injection of pentobarbital (35mg/kg). The T8-T9 vertebrae were exposed by laminectomy using a pair of fine rongeurs, and the dura mater was protected. Spinal crush injury was inflicted at the T8–T9 segment by lateral compression using Dumont-type forceps at the depth of 0.2 mm for 20s. The mice were intramuscularly injected with 20,000 units of penicillin after the operation, and then intraperitoneally with SC79 (40mg/kg in DMSO) or BAY87-2243 (0.5mg/kg and 4mg/kg in DMSO) every day after SCI. The control mice were injected with the same volume of DMSO at the same time points.

Locomotion recover assessment

The locomotive behavior after SCI was assessed by the Basso Mouse Scale (BMS) locomotor recovery scale, which scores ankle movement, plantar placement, weight support, stepping, coordination, paw position and trunk stability from 0 (no spontaneous movement) to 9 (normal coordinated gait with parallel paw placement). The mice were examined on 1, 3, 7, 14, 21 and 28 days post-operation by an investigator blinded to the grouping in an open field.

Cell cultures

BV2 cells were cultured in DMEM (Gibco, Carlsbad, CA, USA) supplemented with 10% FBS (Gibco, Carlsbad, CA, USA), 50 g/ml streptomycin (Invitrogen, Carlsbad, CA, USA) and 50 U/ml penicillin in a humidified atmosphere of 95% air and 5% CO_2. RNAi-CD73, pcDNA-CD73 and RNAi-HIF-1 were constructed by Genechem Co. Ltd. (Shanghai, China), and transfected into BV2 cells using Lipofectamine™ 2000 reagent (Invitrogen, Carlsbad CA, USA) according to the manufacturer's instructions. Different combinations of LPS (1μg/ml), adenosine (10μM), MRS1706 (0.3μM) and MK2206 (3μM) were added to the media 24h after transfection, and cells were harvested 8h later.

RNA sequencing and functional enrichment analysis

Total RNA was isolated from cultured cells using Trizol (Invitrogen□Carlsbad CA, USA) according to the manufacturer's protocol, and their quality was assessed using the Agilent 2200 TapeStation (Agilent Technologies, USA). The purified RNAs with RIN score > 7 were reverse transcribed into cDNA, followed by adaptor ligation and enrichment using NEBNext® Ultra™ RNA Library Prep Kit for Illumina (NEB, USA) as per the manufacturer's instructions. The purified library constructs were evaluated using the Agilent 2200 TapeStation and Qubit®2.0 (Life Technologies, USA) and then diluted to 10pM for cluster generation *in situ* on the pair-end flow cell followed by HiSeq3000 sequencing (2×150 bp). The clean reads were obtained after removing those containing adapters and ploy-N, as well as the low quality reads. HISAT2

was used to align the clean short reads to the mouse reference genome mm10 with default parameters, and converted into read counts for each gene model using HTSeq. The differentially expressed genes (DEGs) were assessed by DEseq using read counts as the input and Benjamini–Hochberg multiple test correction, with fold change > 2 and adjusted p-value < 0.05 as the cut-offs. The DEGs were displayed by a heat map and subjected to KEGG enrichment analysis using p-value < 0.05 as the threshold.

Enzyme-linked immunosorbent assay

IL-1β, IL-6 and TNF-α levels in cell culture supernatants and mouse spinal cord homogenates were measured using commercial ELISA kits from Sigma (Sigma-Aldrich, St. Louis, MO, USA) according to the manufacturer's instructions.

Cytotoxicity assay

The amount of lactate dehydrogenase (LDH) released by the suitably-treated cells was measured using the LDH Cytotoxicity Assay Kit (Beyotime, Shanghai, China) following the manufacturer's instructions.

Western blotting

Spinal cord tissues and BV2 cells were homogenized in radioimmunoprecipitation assay (RAPI) lysis buffer, and protein concentration was determined using the BCA assay. Equal amounts of protein per sample were fractionated by sodium dodecyl sulfate-polyacrylamide gel electrophoresis (SDS-PAGE), and transferred to nitrocellulose membranes. After blocking for 1h with 5% skimmed milk in TBST, the membranes were incubated overnight with antibodies targeting NLRP3 (1:1000, Abcam, ab214185), PI3K (1:1000, CST, 4228), AKT (1:1000, CST, 2920), p-AKT (1:1000, CST, 4070), Foxo1 (1:1000, CST, 14952), p-Foxo1 (1:1000, CST, 9641), GSDMD (1:1000, Abcam, ab210070), ASC (1:1000, CST, 67824) and GAPDH (1:2000, Abcam, ab8245) at 4°C. After washing with TBST, the membranes were incubated with HRP-conjugated secondary antibody at room temperature for 1h, and the positive bands were detected using an enhanced chemiluminescence (ECL) kit and quantified by a gel imaging system (UVP LLC, Upland, CA, USA).

Immunohistochemistry

On the third day after SCI, the mice were deeply anesthetized with 10% chloralic hydras (3.5 ml/kg, i.p.), and sequentially perfused with 0.9% NaCl and 4% paraformaldehyde in 0.01M PBS. The spinal cord segments near the lesion epicenter were resected, embedded in paraffin, cut into 25μm-thick transverse sections, and mounted on poly-L-lysine coated slides. The sections were deparaffinized, incubated with H_2O_2 and methanol for 10 min to block endogenous peroxidase, and blocked with serum for 30 min. The sections were incubated sequentially with primary antibodies against CD73 (1:100, Abcam, ab175396), GSDMD (1:100, Abcam, ab210070) and CASP-1 (1:100, Abcam, ab1872) for 1h, followed by HRP-conjugated anti-rabbit secondary antibody for 30 min. Following color development with DAB for 10 min,

the slides were observed under a Nikon ECLIPSE Ti microscope (Nikon, Japan). Semi-quantification of integrated optical density (IOD) and area was done with the help of Image Pro Plus 6.0.

Immunofluorescence

Spinal cord tissue samples were harvested as described above, and the suitably-treated BV2 cells were fixed with 4% paraformaldehyde in 0.1M PBS for 15 min. The samples were blocked for 1h with 1% bovine serum albumin containing 0.3% Triton X-100, followed by overnight incubation with anti-GSDMD (1:100, Abcam, ab210070) and anti-CASP-1 (1:100, Abcam, ab1872) primary antibodies at 4°C. After incubating with Dylight (Dy)488- and Dy594-conjugated secondary antibodies (all 1:1000; Jackson ImmunoResearch, West Grove, PA) for 2h at room temperature, the slides were observed under the Nikon ECLIPSE Ti microscope (Nikon, Japan).

Promoter cloning and dual-luciferase reporter assay

The -2000/+200bp region of murine GSDMD promoter was cloned from C57BL/6J mouse genomic DNA and inserted into the pGL3 basic vector (Promega, Madison, WI, USA). Truncated GSDMD promoter sequences were generated with -1450/+200bp, -900/+200bp, -300/+200bp and +50/+200bp deletions. Mutant GSDMD promoter sequences were further generated using the -300/+200bp construct. BV2 cells were co-transfected with the luciferase reporter plasmids or pRL-TK reporter plasmid (control), and the FOXO1 plasmid (pc-FOXO1). The cells were harvested 24h after transfection and luciferase activity was measured using toolVeritas 9100-002 (Turner BioSystems, Sunnyvale, CA, USA), and normalized to Renilla luciferase activity.

Chromatin immunoprecipitation assay

ChIP assay was performed using a ChIP assay kit (Abcam, Cambridge, UK) according to the manufacturer's protocol. Briefly, the cells were incubated with primary antibodies against FOXO1 (1:500, CST, 2880) or IgG (1:500, Abcam, ab172730), and the DNA–protein cross-linked complexes were precipitated. The DNA was purified and subjected to qPCR using SYBR Green PCR Master Mix (ThermoFisher, CA, USA).

Statistical analysis

All data were expressed as mean ± standard deviation, and compared by Student's unpaired t tests and two-way analysis of variance (ANOVA) followed by Dunnett's test. $P < 0.05$ was considered statistically significant. The associations between CD73/GSDMD expression and the clinicopathological characteristics of the patients were analyzed using the Chi-squared test. All statistical analyses were performed using SPSS 14.0 software.

Results

NLRP3 and GSDMD are overexpressed in the peripheral blood of SCI patients and positive correlated with disease severity

As shown in Fig. 1A-B, NLRP3/GSDMD mRNA levels were significantly higher in the peripheral blood of SCI patients compared to the healthy controls. The patients were accordingly classified into the high- and low-expression groups based on the average expression level. Patients overexpressing NLRP3/GSDMD had a higher NDI index compared to the low-expression group (Table 1). Furthermore, a negative correlation between CD73/GSDMD expression and NDI index (Fig. 1C-1D). Finally, ROC curves demonstrated considerable diagnostic accuracy of NLRP3 and GSDMD for SCI (Fig. 1E). Taken together, both factors play key roles in SCI, and correlate significantly with disease severity.

CD73 deficiency activates NLRP3 inflammasome and promotes microglia pyroptosis *in vivo*

The inflammasome-associated markers including IL-1β, IL-18, CASP-1 and GSDMD (Supplementary Fig. 1A), as well as sensors like NLRP3 and AIM2 (Supplementary Fig. 1B) were elevated in the damaged spinal cords within 3 days of SCI induction. Compared to the WT mice however, the CD73 KO mice had significantly higher *in situ* levels of the above factors 3 days post injury (Fig. 2A-2B), which corresponded to increased secretion of IL-1β, IL-6, TNF-α and LDH (Fig. 2C-2D). The protein expression patterns of NLRP3, GSDMD, ASC and CASP-1 were consistent with that of their transcripts (Fig. 2E-2F, 2H). Furthermore, CD73 deficiency increased the levels of both full length GSDMD and the cleaved active N-terminal GSDMD (GSDMD-N) (Fig. 2E-2F), which co-localized with the microglial marker CD68 (Fig. 2G). Taken together, lack of CD73 exacerbates post-SCI pyroptosis in the microglia by activating the NLRP3 inflammasome.

CD73 alleviates inflammasome activation and microglia pyroptosis via the A_{2B}AR/ PI3K/AKT/FOXO1 pathway

In a previous study, we found that CD73 blocked microglial polarization through the A_{2B} adenosine receptor (A_{2B}AR). To determine whether A_{2B}AR also mediates the anti-pyroptotic effect of CD73, we generated BV2 cell lines with stable CD73 knockdown or overexpression, and treated them with adenosine or the A_{2B}AR antagonist MRS1706 following LPS stimulation. CD73 knockdown induced pyroptosis genes including NLRP3, ASC, CASP-1 and GSDMD, and increased secretion of IL-1β, IL-6, TNF-α and LDH, whereas CD73 upregulation had the opposite effects (Fig. 3A-3F). Interestingly, adenosine and MRS1706 respectively abrogated the effects of CD73 knockdown and overexpression (Fig. 3A-3F). Taken together, A_{2B}AR is necessary for CD73-mediated inhibition of microglia pyroptosis.

Furthermore, mRNA sequencing of the LPS-stimulated WT and $CD73^{hi}$ BV2 cells revealed 1649 DEGs (Fig. 4A), of which 1081 were upregulated and 568 were downregulated. Furthermore, 55 DEGs were enriched in the PI3K/AKT pathway (Fig. 4B). Consistent with this, PI3K was upregulated in the CD73-overexpressing cells, which was accompanied by increased phosphorylation of AKT and FOXO1 (Fig. 4C-4E). MRS1706 and the AKT antagonist MK2206 significantly downregulated PI3K, p-AKT and p-FOXO1 in

the CD73-overexpressing cells (Fig. 4C-4E), and concomitantly upregulated the inflammasome genes and increased secretion of pro-inflammatory factors (Fig. 4F-4J). Consistent with this, CD73-KO mice injected with the AKT activator SC79 following injury showed lower expression of GSDMD and CASP-1 at the lesion site (Fig. 4K), and improved BBB scores compared to the DMSO-injected controls on the 28th day after surgery (Fig. 4L). Taken together, CD73 inhibits microglial pyroptosis via the PI3K/AKT/FOXO1 pathway.

FOXO1 is a transcriptional activator of GSDMD

To further dissect the molecular mechanisms involved in GSDMD regulation, we screened for putative POXO1 binding sites in its promoter region through the JASPAR database (http://jaspar.genereg.net), and identified 3 cis-acting elements. The exact regulatory sequence was determined using 5 reporters constructs with progressively larger deletions from the 5' end of the GSDMD promoter. Dual luciferase assay showed increased promoter activity of the pGL3–2000/+ 200bp construct in BV2 cells, indicating a FOXO1 binding site within this region (Fig. 5A), which was also confirmed by ChIP assay (Fig. 5B). Furthermore, a significant decrease in promoter activity of pGL3+50/+200bp compared to pGL3–300/+200 further narrowed the regulatory elements in the −300/+50 region (Fig. 5A). Further mutations in this binding site blocked GSDMD transcription (Fig. 5C), which validated FOXO1 binding to the promoter. Consistent with this, FOXO1 overexpression in BV2 cells upregulated GSDMD. Ectopic expression of both FOXO1 and CD73 plasmid inhibited GSDMD mRNA, and reduced the secretion of IL-1β, IL-6, TNF-α and LDH (Fig. 5D-5F). Taken together, FOXO1 regulates the expression of GSMDM at the transcriptional level.

HIF-1α upregulates CD73 in the microglia

Consistent with previous studies, LPS-induced pyroptosis in BV2 cells significantly increased the expression of HIF-1α and CD73, and siRNA-mediated silencing of HIF-1α downregulated CD73 (Fig. 6A-C). Furthermore, the spinal cord lesions in the injured mice also showed increased expression of both HIF-1α and CD73, which was reversed by treating the mice with the HIF-1α inhibitor BAY87-2243 (Fig. 6D-G). Since BAY87-2243 primarily targets HIF-1α activity, wee hypothesized that the decrease in HIF-1α mRNA and protein levels (Fig. 6D-F) was a result of CD73 downregulation. Indeed, CD73-knockdown BV2 cells and CD73-KO mice did not show an increase in HIF-1α even after LPS stimulation or SCI respectively (Fig. 7A-F). Merighi et al. reported an A_{2B}AR-dependent stimulatory effect of adenosine on HIF-1α via p38 mitogen-activated protein kinases (MAPKs) phosphorylation [25]. Furthermore, we previously found that CD73 regulates the polarization of macrophages/microglia through this pathway [24]. Consistent with this, MRS1706 or the p38 inhibitor SB203580 neutralized CD73-driven increase in HIF-1α in BV2 cells (Fig. 7G-8I). Taken together, HIF-1α and CD73 synergistically promote microglial pyroptosis.

Discussion

CNS trauma such as SCI and traumatic brain injury (TBI) show a biphasic progression, namely primary and secondary injury, depending on the pathological characteristics [26]. Secondary injury is persistent and diffuse, and is characterized by delayed glial and neuronal death, which expands the damaged site and can lead to progressive neurodegeneration [27][28]. Neuroinflammation initiated by the innate immune response is a key pathological factor in the secondary injury after CNS trauma, and is therefore a promising therapeutic target [2][6]. An essential step in secondary CNS damage is pyroptosis due to activation of the cytoplasmic inflammasome complex [7]. We detected significantly higher levels of the inflammasome and pyroptosis-related proteins NLRP3 and GSDMD in the blood of SCI patients, which also correlated with disease severity. Consistent with our previous study, the 5'-ecto-nucleotidase CD73 attenuated neuroinflammation and microglia pyroptosis in both *in vitro* and *in vivo* models of SCI. Our findings provide novel insights into the patho-molecular basis of SCI, as well as new therapeutic possibilities.

Inflammasome complexes consist of a cytosolic pattern-recognition receptor, a pro-inflammatory caspase and the adaptor protein ASC that facilitates the interaction between the first two proteins [11], [29]. The NLRP3 complex is frequently involved in CNS trauma [30], and is overexpressed in the microglia, neurons and astrocytes of rats with TBI [31]. Wu et al showed that pharmacological suppression of NLRP3 attenuated neuroinflammation and mitochondrial dysfunction in mice [19]. In addition, Adamczek et al reported activation of AIM2 in the cortical neurons in response to TBI [32]. Consistent with this, we found that both NLRP3 and AIM2 were overexpressed in the murine spinal cord tissues after compression injury. To determine the role of CD73 in SCI, we compared the transcriptomic profiles of WT and CD73-KO mice, and detected overexpression of inflammasome genes in the latter. We surmised therefore that CD73 also plays a crucial role in regulating NLRP3-driven pyroptosis after SCI.

Macrophages/microglia are the primary cellular mediators of the innate immune responses and neuroinflammation following CNS trauma [33][34]. In addition, these cells are also the major sites of pyroptosis in neuro-immunological diseases. This is likely due to the high surface expression of PRRs that can recognize PAMPs and DAMPs, and initiate the pyroptosis cascade [10][18]. Consistent with this, we detected high levels of GSDMD in the microglia of spinal cord lesions in CD73-KO mice, indicating that CD73 inhibits microglial pyroptosis post SCI.

CD73 is a glycosylphosphatidylinositol (GPI)-anchored cell surface protein with a central role in the adenosinergic system, and is the rate-limiting enzyme in extracellular adenosine biogenesis [35]. Kulesskaya et al. found about 85–95% of murine AMP is hydrolyzed by CD73 [36]. Elevated extracellular adenosine activates the P1 purinergic receptors (adenosine receptors) on target cells and stimulates protective cellular responses [37][38]. The P1 G-protein-coupled receptor family consists of the A_1R, $A_{2A}R$, $A_{2B}R$ and A_3R subtypes [39], which have different affinities for adenosine. A_1R, $A_{2A}R$ and A_3R are the high-affinity receptors that can be activated by physiological adenosine levels, while $A_{2B}R$ can only be activated under pathological/inflammatory conditions [40][41]. Hypoxia-mediated upregulation of $A_{2B}R$ [42] plays a protective role in rat lung injury [43] and myocardial ischemia [44]. It also mediates the

protective effects of CD73 in the mouse model of SCI [24]. Thus, the CD73/adenosine/A_{2B}R cascade may also be involved in microglial pyroptosis after SCI. Indeed, the effect of CD73 silencing or overexpression in BV2 cells was respectively counteracted by adenosine and MRS1706.

KEGG pathway analysis of the DEGs between the LPS-stimulated control and CD73-overexpressing BV2 cells showed a significant enrichment in the PI3K/AKT pathway. This pathway plays a central role in multiple cellular functions such as cell proliferation and survival [45], and its activation is closely related to the inflammatory response. Yin et al. showed that the expression of pro-inflammatory factors like IL‐12, TNF‐α and IL‐6 was increased in human innate immune cells by PI3K or AKT inhibitors, while that of the anti-inflammatory factor IL‐10 was decreased [46]. Another study showed that AKT activation inhibited the inflammatory responses during LPS-induced sepsis in mice and rabbits [47]. Therefore, the PI3K/AKT pathway has an immunosuppressive function similar to that of CD73. Constitutive activation of the PI3K/AKT pathway results in the phosphorylation and nuclear translocation of the transcription factor FOXO1, which activates pro-inflammatory genes [48]. Although FOXO1 inhibition alleviated inflammation in different cells [49],[50], no study so far has associated FOXO1 with CD73 or pyroptosis. We found that not only did CD73 overexpression alleviate pyroptosis in macrophages/microglia via the PI3K/AKT pathway, but the GSDMD promoter harbored a FOXO1 binding site as well. Based on the above findings, the PI3K/AKT/Foxo1 pathway is essential for CD73-mediated inhibition of pyroptosis.

HIF-1 is a heterodimeric transcription factor composed of HIF-1α and HIF-1β subunits, and is a master regulator of oxygen homeostasis [51]. Under anoxic conditions, the HIF-1α subunit accumulates and then binds to HIF-1β, which activates the HIF-1-target genes regulating angiogenesis, glucose metabolism, cell survival, invasion and metastasis [52]. SCI pathogenesis involves ischemia and hypoxia at the lesion site, which upregulates HIF-1 and enhances the resilience of neuronal cells under hypoxia [53],[54]. Karhausen et al. found that HIF-1α transcriptionally activated CD73 in colitis, which attenuated loss of barrier [55]. In addition, Synnestvedt et al. identified a HIF-1α binding site in the CD73 gene promoter, and inhibition of HIF-1α by antisense oligonucleotides significantly decreased hypoxia-inducible CD73 expression [56]. Consistent with this, CD73 and HIF-1α expression levels in the injured spinal cord were dependent on each other. Furthermore, CD73 regulated HIF-1α via the adenosine-A_{2B}AR-p38 pathway, which is consistent with the findings of Merighi et al [25]. Therefore, we hypothesize a positive feedback regulatory loop between CD73 and HIF-1α after SCI, which regulated macrophages/microglia pyroptosis and inhibits neuroinflammation.

A limitation can’t be neglected in this study is the alternative of BV2 cell line as primary microglia. BV2 cells were derived from raf/myc-immortalised murine neonatal microglia and are the most frequently used substitute for primary microglia. Although there exits research confirmed BV2 cells appear to be a valid substitute for primary microglia in many experimental settings including complex cell-cell interaction studies [57], however, doubts have been raised that this cell line does not always model the reaction of primary microglia[58][59]. Therefore, although the present study is helpful in understanding the mechanism of microglial pyroptosis, further experimental verification is still needed.

Conclusion

CD73 may attenuate post-SCI pyroptosis by inhibiting GSDMD via the adenosine- A_{2B}AR-PI3K-AKT-FOXO1 pathway. A positive feedback loop between CD73 and HIF-1α is another potential mechanism that reduces neuroinflammation after SCI (Fig. 8). Thus, CD73 may be a novel therapeutic target for SCI.

Abbreviations

GSDMD: gasdermin D, SCI: Spinal cord injury, CNS: central nervous system, PRRs: pattern recognition receptors, PAMPs: pathogen-associated molecular patterns, DAMPs: damage-associated molecular patterns, DEGs: differentially expressed genes, NDI: cervical dysfunction index, ASIA: American spinal injury association.

Declarations

Acknowledgements

The authors thank Prof. Thompson (Oklahoma Medical Research Foundation, Oklahoma City, USA) for the CD73 deficient mice.

Funding

This work was supported by the National Natural Science Foundation of China [grant number 81772385, 81871522].

Availability of supporting data

All data generated or analyzed during this study are included in this published article.

Author Contributions

Shun Xu, Wei Zhu, Minghao Shao, Fan Zhang, Haocheng Xu performed the experiments; Feizhou Lu, Wei Zhu, Xiaosheng Ma, and Shun Xu designed the study; Shun Xu analyzed the data and wrote the manuscript. Feizhou Lu, Jianyuan Jiang, Xiaosheng Ma reviewed and edited the manuscript. All authors read and approved the final manuscript.

Ethics, consent and permissions

All study surgical procedures and experiment protocols have been approved by the Ethics Committee of Experimental Research, Shanghai Medical College, Fudan University (NO: 2019-JS-053). All participants have been informed the potential risks and benefits of the study, and each patient has signed an informed consent form before blood sample collection.

Consent to publish

All participants agree to publish.

Conflict of interest

We declare that we do not have any commercial or associative interest that represents a conflict of interest in connection with the work submitted.

References

1. Singh A, Tetreault L, Kalsi-Ryan S, Nouri A, Fehlings MG. Global prevalence and incidence of traumatic spinal cord injury. Clin Epidemiol. 2014;6:309–31.
2. Putatunda R, Bethea JR, Hu W-H. Potential immunotherapies for traumatic brain and spinal cord injury. Chinese J Traumatol. 2018;21:125–36.
3. Mortazavi MM, Verma K, Harmon OA, Griessenauer CJ, Adeeb N, Theodore N, et al. The microanatomy of spinal cord injury: A review. Clin Anat. 2015;28:27–36.
4. Beck KD, Nguyen HX, Galvan MD, Salazar DL, Woodruff TM, Anderson AJ. Quantitative analysis of cellular inflammation after traumatic spinal cord injury: evidence for a multiphasic inflammatory response in the acute to chronic environment. Brain. 2010;133:433–47.
5. Hayden MS, Ghosh S. NF-κB in immunobiology. Cell Res. 2011;21:223–44.
6. Wang Y-T, Lu X-M, Chen K-T, Shu Y-H, Qiu C-H. Immunotherapy strategies for spinal cord injury. Curr Pharm Biotechnol. 2015;16:492–505.
7. Mortezaee K, Khanlarkhani N, Beyer C, Zendedel A. Inflammasome: Its role in traumatic brain and spinal cord injury. J Cell Physiol. 2018;233:5160–9.
8. McKee CA, Lukens JR. Emerging Roles for the Immune System in Traumatic Brain Injury. Front Immunol. 2016;7:556.
9. Zendedel A, Johann S, Mehrabi S, Joghataei M, Hassanzadeh G, Kipp M, et al. Activation and Regulation of NLRP3 Inflammasome by Intrathecal Application of SDF-1a in a Spinal Cord Injury Model. Mol Neurobiol. 2016;53:3063–75.
10. Vande Walle L, Lamkanfi M. Pyroptosis. Curr Biol. 2016;26:R568–72.

11. Broz P, Dixit VM. Inflammasomes: mechanism of assembly, regulation and signalling. Nat Rev Immunol. 2016;16:407–20.
12. Aglietti RA, Estevez A, Gupta A, Ramirez MG, Liu PS, Kayagaki N, et al. GsdmD p30 elicited by caspase-11 during pyroptosis forms pores in membranes. Proc Natl Acad Sci. 2016;113:7858–63.
13. Shi J, Zhao Y, Wang K, Shi X, Wang Y, Huang H, et al. Cleavage of GSDMD by inflammatory caspases determines pyroptotic cell death. Nature. 2015;526:660–5.
14. Liu X, Zhang Z, Ruan J, Pan Y, Magupalli VG, Wu H, et al. Inflammasome-activated gasdermin D causes pyroptosis by forming membrane pores. Nature. 2016;535:153–8.
15. Aglietti RA, Dueber EC. Recent Insights into the Molecular Mechanisms Underlying Pyroptosis and Gasdermin Family Functions. Trends Immunol. 2017;38:261–71.
16. Zhang Y, Chen X, Gueydan C, Han J. Plasma membrane changes during programmed cell deaths. Cell Res. 2018;28:9–21.
17. David S, Greenhalgh AD, Kroner A. Macrophage and microglial plasticity in the injured spinal cord. Neuroscience. 2015;307:311–8.
18. Walsh JG, Muruve DA, Power C. Inflammasomes in the CNS. Nat Rev Neurosci. 2014;15:84–97.
19. Jiang W, Li M, He F, Zhou S, Zhu L. Targeting the NLRP3 inflammasome to attenuate spinal cord injury in mice. J Neuroinflammation. 2017;14:207.
20. Liu W, Chen Y, Meng J, Wu M, Bi F, Chang C, et al. Ablation of caspase-1 protects against TBI-induced pyroptosis in vitro and in vivo. J Neuroinflammation. 2018;15:48.
21. Antonioli L, Pacher P, Vizi ES, Haskó G. CD39 and CD73 in immunity and inflammation. Trends Mol Med. 2013;19:355–67.
22. Yu J, Wang X, Lu Q, Wang J, Li L, Liao X, et al. Extracellular 5'-nucleotidase (CD73) promotes human breast cancer cells growth through AKT/GSK-3β/β-catenin/cyclinD1 signaling pathway. Int J Cancer. 2018;142:959–67.
23. Bynoe MS, Waickman AT, Mahamed DA, Mueller C, Mills JH, Czopik A. CD73 Is Critical for the Resolution of Murine Colonic Inflammation. J Biomed Biotechnol. 2012;2012:1–13.
24. Xu S, Zhu W, Shao M, Zhang F, Guo J, Xu H, et al. Ecto-5'-nucleotidase (CD73) attenuates inflammation after spinal cord injury by promoting macrophages/microglia M2 polarization in mice. J Neuroinflammation. 2018;15:155.
25. Merighi S, Borea PA, Stefanelli A, Bencivenni S, Castillo CA, Varani K, et al. A 2a and a 2b adenosine receptors affect HIF-1α signaling in activated primary microglial cells. Glia. 2015;63:1933–52.
26. Sekhon LHS, Fehlings MG. Epidemiology, demographics, and pathophysiology of acute spinal cord injury. Spine (Phila Pa 1976). 2001;26:S2-12.
27. Lin W-P, Xiong G-P, Lin Q, Chen X-W, Zhang L-Q, Shi J-X, et al. Heme oxygenase-1 promotes neuron survival through down-regulation of neuronal NLRP1 expression after spinal cord injury. J Neuroinflammation. 2016;13:52.

28. Lozano D, Gonzales-Portillo GS, Acosta S, de la Pena I, Tajiri N, Kaneko Y, et al. Neuroinflammatory responses to traumatic brain injury: etiology, clinical consequences, and therapeutic opportunities. Neuropsychiatr Dis Treat. 2015;11:97–106.
29. Rathinam VAK, Fitzgerald KA. Inflammasome Complexes: Emerging Mechanisms and Effector Functions. Cell. 2016;165:792–800.
30. Wallisch JS, Simon DW, Bayır H, Bell MJ, Kochanek PM, Clark RSB. Cerebrospinal Fluid NLRP3 is Increased After Severe Traumatic Brain Injury in Infants and Children. Neurocrit Care. 2017;27:44–50.
31. Liu H-D, Li W, Chen Z-R, Hu Y-C, Zhang D-D, Shen W, et al. Expression of the NLRP3 Inflammasome in Cerebral Cortex After Traumatic Brain Injury in a Rat Model. Neurochem Res. 2013;38:2072–83.
32. Adamczak SE, de Rivero Vaccari JP, Dale G, Brand FJ, Nonner D, Bullock M, et al. Pyroptotic Neuronal Cell Death Mediated by the AIM2 Inflammasome. J Cereb Blood Flow Metab. 2014;34:621–9.
33. David S, Kroner A. Repertoire of microglial and macrophage responses after spinal cord injury. Nat Rev Neurosci. 2011;12:388–99.
34. Loane DJ, Byrnes KR. Role of microglia in neurotrauma. Neurotherapeutics. 2010;7:366–77.
35. Resta R, Yamashita Y, Thompson LF. Ecto-enzyme and signaling functions of lymphocyte CD73. Immunol Rev. 1998;161:95–109.
36. Kulesskaya N, Võikar V, Peltola M, Yegutkin GG, Salmi M, Jalkanen S, et al. CD73 Is a Major Regulator of Adenosinergic Signalling in Mouse Brain. Eckle T, editor. PLoS One. 2013;8:e66896.
37. Csóka B, Haskó G. Adenosine, inflammation pathways and therapeutic challenges. Jt Bone Spine. 2011;78:4–6.
38. Phillis JW, Goshgarian HG. Adenosine and neurotrauma: Therapeutic perspectives. Neurol Res. 200;23:183–9.
39. Fredholm BB, IJzerman AP, Jacobson KA, Klotz KN, Linden J. International Union of Pharmacology. XXV. Nomenclature and classification of adenosine receptors. Pharmacol Rev. 2001;53:527–52.
40. Haskó G, Linden J, Cronstein B, Pacher P. Adenosine receptors: therapeutic aspects for inflammatory and immune diseases. Nat Rev Drug Discov. 2008;7:759–70.
41. Ohta A, Sitkovsky M. Role of G-protein-coupled adenosine receptors in downregulation of inflammation and protection from tissue damage. Nature. 2001;414:916–20.
42. Boros D, Thompson J, Larson D. Adenosine regulation of the immune response initiated by ischemia reperfusion injury. Perfusion. 2016;31:103–10.
43. Eckle T, Grenz A, Laucher S, Eltzschig HK. A2B adenosine receptor signaling attenuates acute lung injury by enhancing alveolar fluid clearance in mice. J Clin Invest. 2008;118:3301–15.
44. Eckle T, Krahn T, Grenz A, Köhler D, Mittelbronn M, Ledent C, et al. Cardioprotection by Ecto-5'-Nucleotidase (CD73) and A 2B Adenosine Receptors. Circulation. 2007;115:1581–90.
45. Fruman DA, Chiu H, Hopkins BD, Bagrodia S, Cantley LC, Abraham RT. The PI3K Pathway in Human Disease. Cell. 2017;170:605–35.

46. Yin H, Zhou H, Kang Y, Zhang X, Duan X, Alnabhan R, et al. Syk negatively regulates TLR4-mediated IFNβ and IL-10 production and promotes inflammatory responses in dendritic cells. Biochim Biophys Acta - Gen Subj. 2016;1860:588–98.
47. Wang L, Lu Y, Zhang X, Zhang Y, Jiang D, Dong X, et al. Mindin is a critical mediator of ischemic brain injury in an experimental stroke model. Exp Neurol. 2013;247:506–16.
48. Link W. Introduction to FOXO Biology. Methods Mol Biol. 2019;1890:1–9.
49. Brown J, Wang H, Suttles J, Graves DT, Martin M. Mammalian Target of Rapamycin Complex 2 (mTORC2) Negatively Regulates Toll-like Receptor 4-mediated Inflammatory Response via FoxO1. J Biol Chem. 2011;286:44295–305.
50. Wang Y, Zhou Y, Graves DT. FOXO Transcription Factors: Their Clinical Significance and Regulation. Biomed Res Int. 2014;2014:1–13.
51. de Lemos ML, de la Torre AV, Petrov D, Brox S, Folch J, Pallàs M, et al. Evaluation of hypoxia inducible factor expression in inflammatory and neurodegenerative brain models. Int J Biochem Cell Biol. 2013;45:1377–88.
52. Semenza GL. Expression of hypoxia-inducible factor 1: mechanisms and consequences. Biochem Pharmacol. 2000;59:47–53.
53. Siddiq A, Aminova LR, Troy CM, Suh K, Messer Z, Semenza GL, et al. Selective Inhibition of Hypoxia-Inducible Factor (HIF) Prolyl-Hydroxylase 1 Mediates Neuroprotection against Normoxic Oxidative Death via HIF- and CREB-Independent Pathways. J Neurosci. 2009;29:8828–38.
54. Nordal RA. Hypoxia and Hypoxia-Inducible Factor-1 Target Genes in Central Nervous System Radiation Injury: A Role for Vascular Endothelial Growth Factor. Clin Cancer Res. 2004;10:3342–53.
55. Karhausen J, Furuta GT, Tomaszewski JE, Johnson RS, Colgan SP, Haase VH. Epithelial hypoxia-inducible factor-1 is protective in murine experimental colitis. J Clin Invest. 2004;114:1098–106.
56. Synnestvedt K, Furuta GT, Comerford KM, Louis N, Karhausen J, Eltzschig HK, et al. Ecto-5'-nucleotidase (CD73) regulation by hypoxia-inducible factor-1 mediates permeability changes in intestinal epithelia. J Clin Invest. 2002;110:993–1002.
57. Henn A, Lund S, Hedtjärn M, Schrattenholz A, Pörzgen P, Leist M. The suitability of BV2 cells as alternative model system for primary microglia cultures or for animal experiments examining brain inflammation. ALTEX. 2009;26:83–94.
58. Butovsky O, Jedrychowski MP, Moore CS, Cialic R, Lanser AJ, Gabriely G, et al. Identification of a unique TGF-β–dependent molecular and functional signature in microglia. Nat Neurosci. 2014;17:131–43.
59. Horvath RJ, Nutile-McMenemy N, Alkaitis MS, DeLeo JA. Differential migration, LPS-induced cytokine, chemokine, and NO expression in immortalized BV-2 and HAPI cell lines and primary microglial cultures. J Neurochem. 2008;107:557–69.

Table

Table 1. Clinical characteristics of patient samples and expression of NLRP3 and GSDMD.

	Total	NLRP3		p value	GSDMD		p value
		High	Low		High	Low	
Patients(n)	20	9	11	-	10	10	-
Sex(n)	20	9	11	0.49	10	10	1
Age(years)	49.7±10.3	51.3±12.1	48.4±9.1	0.54	51.9±11.5	57.5±9.1	0.36
Weight(kg)	66.9±7.6	69.2±5.8	64.9±8.6	0.22	67.4±7.9	66.3±7.7	0.76
NDI	35.6±3.9	38.2±3.9	33.6±2.2	0.03	37.9±3.9	33.2±5.3	0.04
ASIA(n)							
a	1	1	0	0.105	1	0	0.306
b	7	5	2		5	2	
c	9	3	6		3	6	
d	3	0	3		1	2	
e	0	0	0		0	0	

Supplementary Figure Legend

Supplementary figure 1. Inflammasome- and pyroptosis-associated genes were up-regulated after SCI (N=3). **A-B.** Relative expression of inflammasome and pyroptosis-related genes in the spinal tissues of mice on the third day after SCI or sham surgery (N=3). *p < 0.05, **p < 0.01, ***p < 0.001. Data are the mean ± SD from 3 independent experiments.

Figures

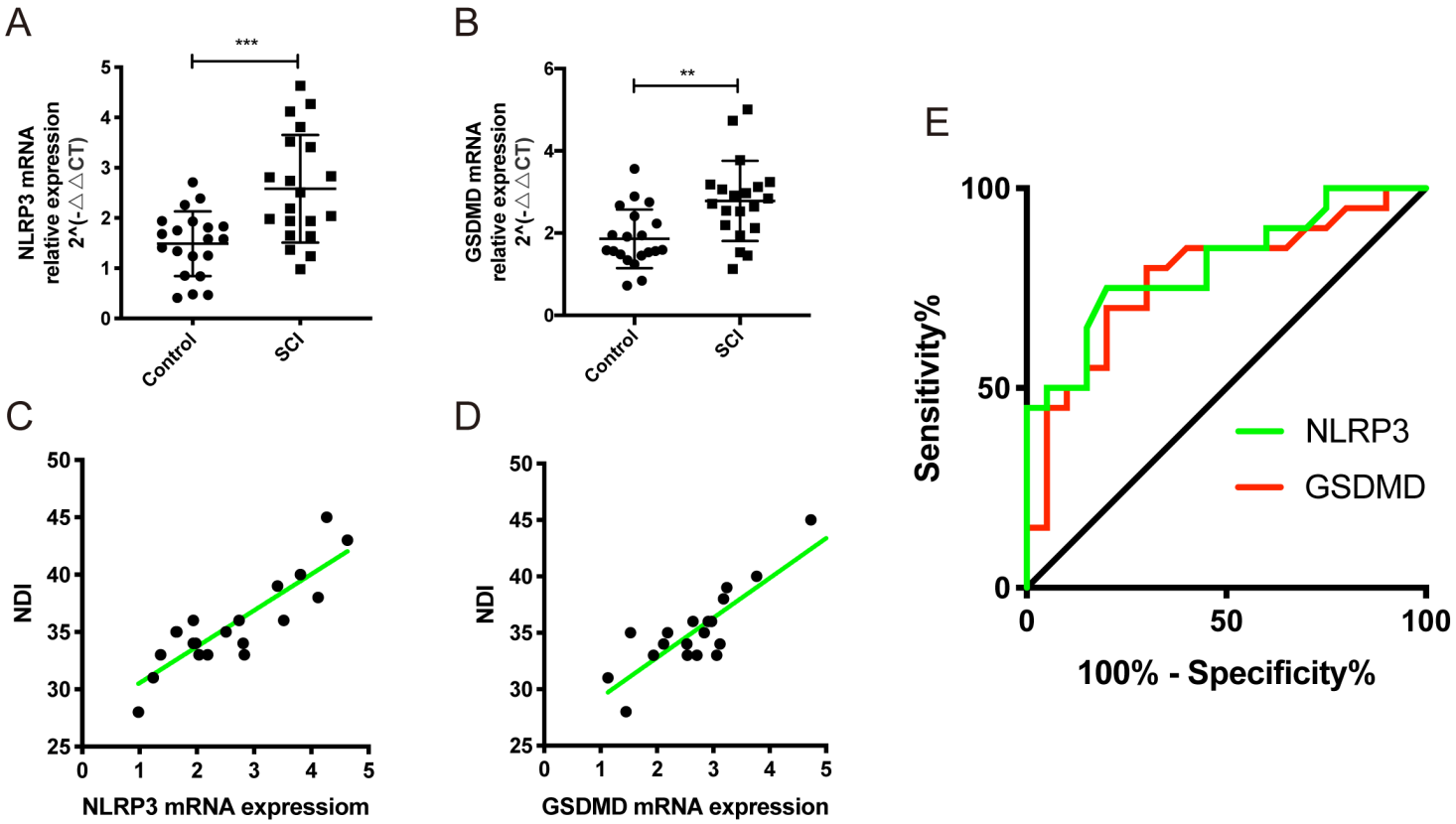

Figure 1

Circulating NLRP3 and GSDMD in SCI patients are correlated with disease severity. A-B. Relative NLRP3 and GSDMD mRNA levels in 20 age- and sex-matched controls and SCI patients. C. Linear regression between NLRP3 mRNA expression and NDI index ($r = 0.86$, $p<0.001$). D. Linear regression between GSDMD mRNA expression and NDI index ($r = 0.87$, $p<0.001$). E. The ROC curve analysis of the diagnostic significance of NLRP3 (AUC=0.74) and GSDMD (AUC=0.72) for SCI.

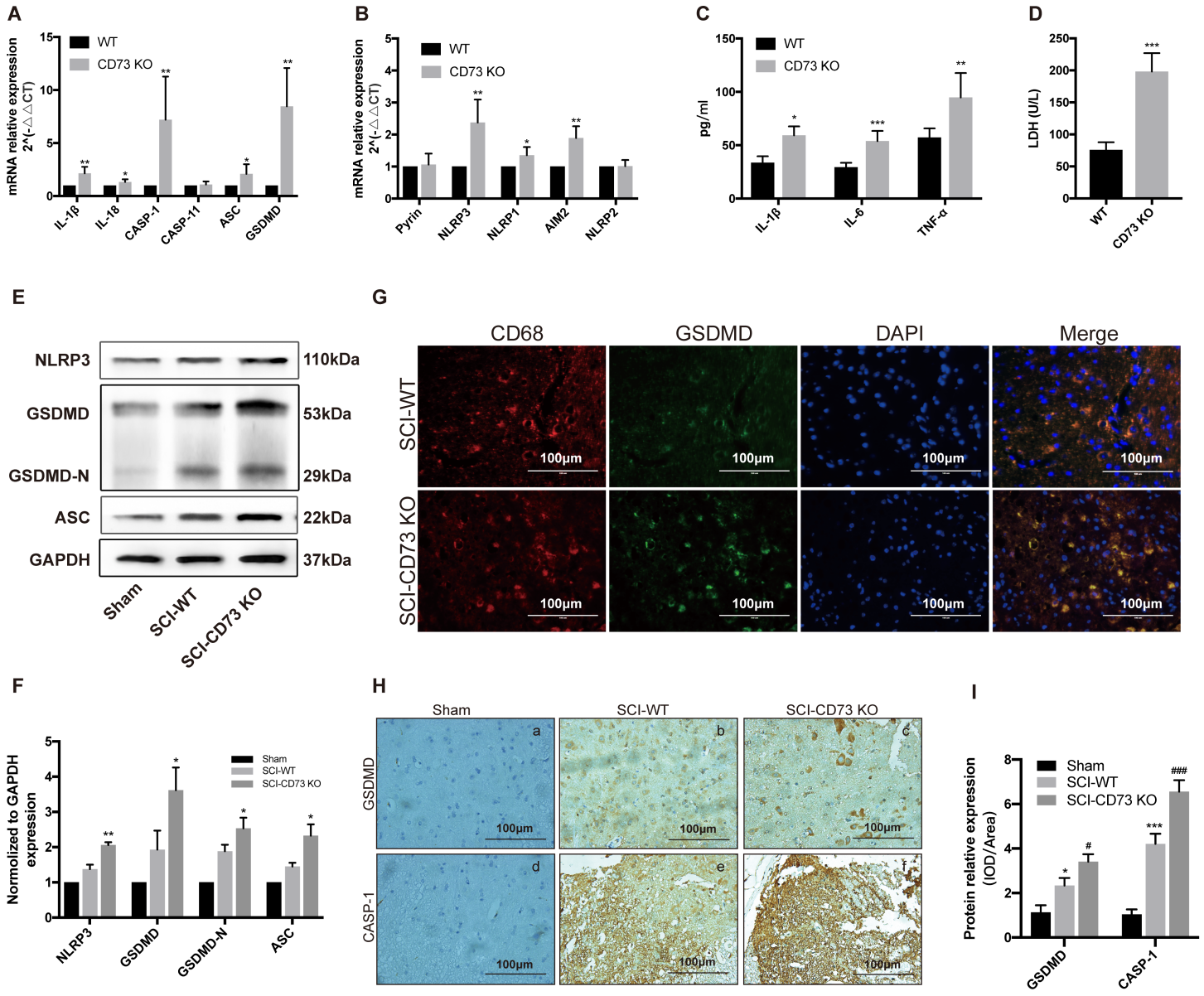

Figure 2

CD73 deficiency facilitates NLRP3 inflammasome activation and pyroptosis in macrophages/microglia in vivo. A-B. Relative expression of pyroptosis-related genes on the third day after SCI in WT and CD73-KO mice (N=3). C. IL-1β, IL-6 and TNF-α levels in the spinal cord homogenates of the above (N=3). D. Secreted LDH levels in the above (N=3). E-F. Representative immunoblots and quantification of pyroptosis-related proteins on the third day after SCI or sham surgery in WT or CD73-KO mice (N=3). G. Representative immunofluorescence images showing in situ expression of CD68 and GSDMD in the spinal tissues of WT or CD73-KO mice 3 days post-injury or sham surgery. H. Representative immunohistochemistry pictures of GSDMD and CASP-1. *p < 0.05, **p < 0.01, ***p < 0.001. Data are the mean ± SD from 3 independent experiments.

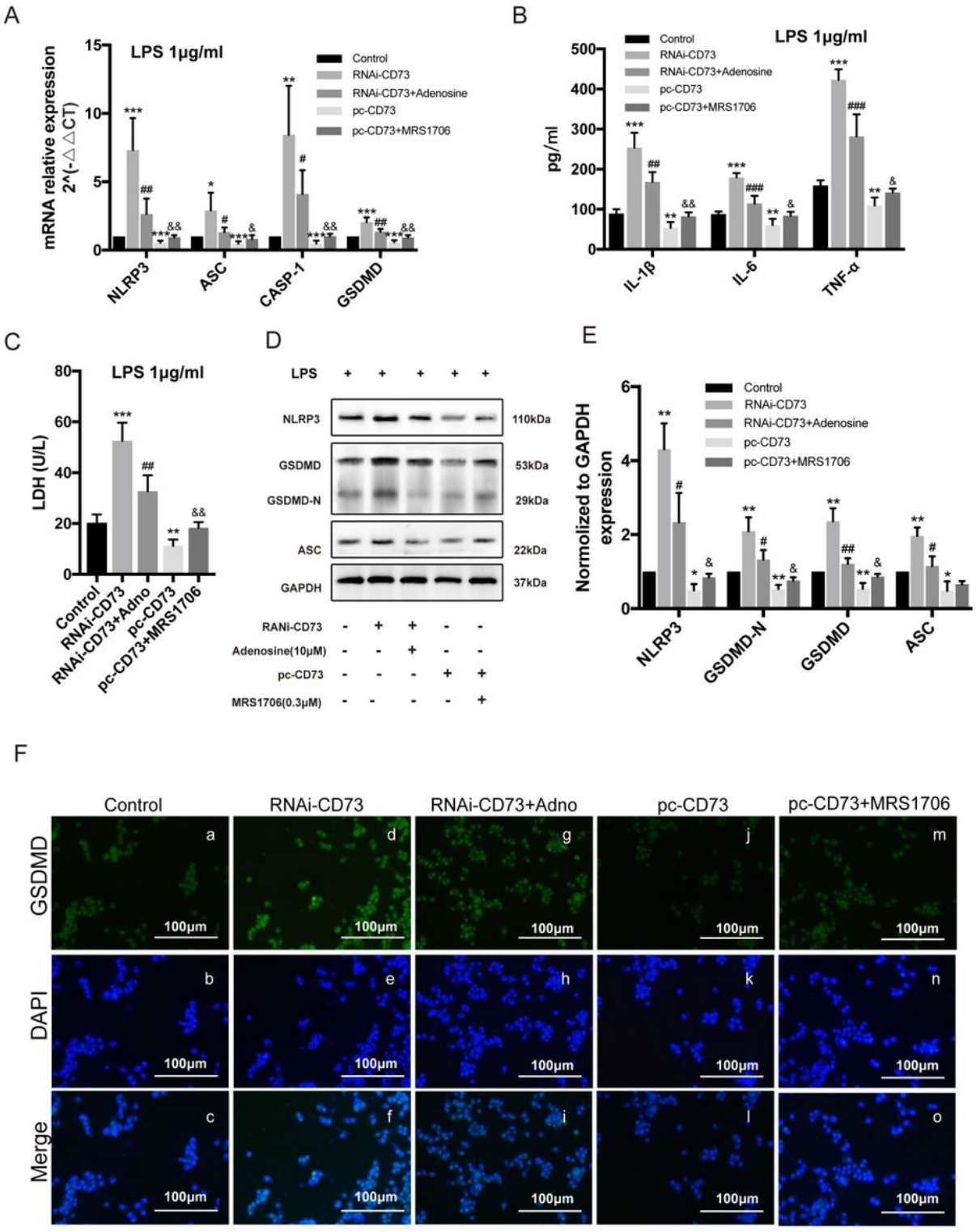

Figure 3

CD73 alleviates LPS-induced NLRP3 inflammasome activation and pyroptosis in microglia through A2BAR. A. NLRP3, ASC, CASP-1 and GSDMD mRNA levels in CD73-overexpressing or knockdown BV2 cells treated with LPS and adenosine or MRS1706 (N=3). B. Amount of IL-1β, IL-6 and TNF-α released by the above treated cells (N=3). C. Secreted LDH levels in the above groups (N=3). D-E. Pyroptosis-related proteins in the differentially-treated BV2 cells (N=3). F. Representative immunofluorescence images

showing in situ expression of GSDMD in the differentially-treated BV2 cells. *p < 0.05, **p < 0.01, ***p < 0.001 versus control; #p < 0.05, ##p < 0.01, ###p < 0.001 versus RNAi-CD73; &p < 0.05, &&p < 0.01 versus pc-CD73. Data are the mean ± SD from 3 independent experiments.

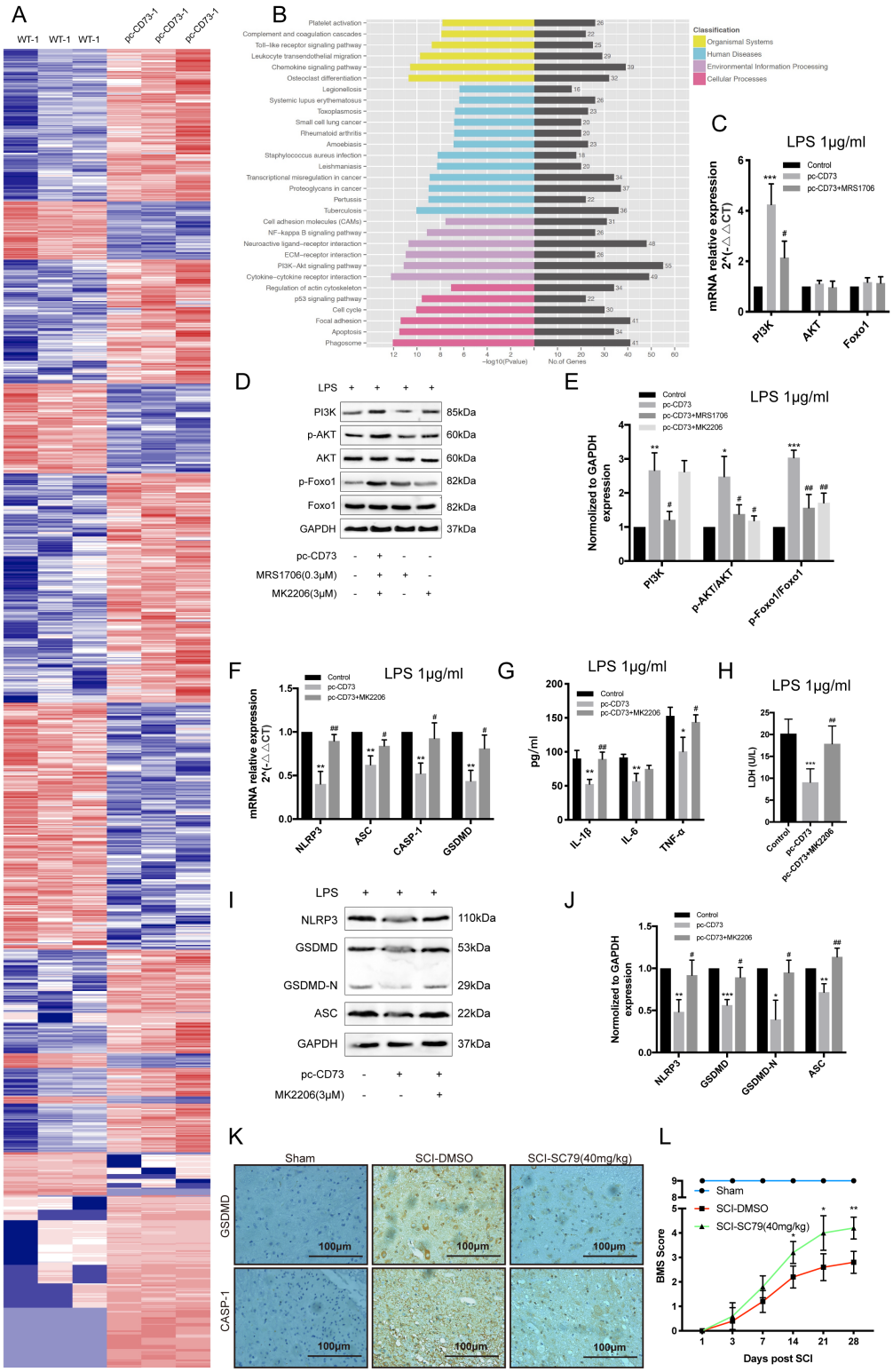

Figure 4

CD73 attenuates microglia pyroptosis via the PI3K/AKT/Foxo1 pathway. A. Heat map showing DEGs between the WT and CD73-overexpressing LPS-stimulated BV2 cells. B. The KEGG pathway analysis of

the DEGs. C. PI3K, AKT and Foxo1 mRNA in BV2 cells challenged with LPS in the presence or absence of pcDNA3.1 or MK2206 (3μM) (N=3). D-E. PI3K, p-PI3K, AKT, p-AKT and FOXO1 protein levels in the differentially-treated BV2 cells (N=3). F. NLRP3, ASC, CASP-1 and GSDMD mRNA levels in CD73-overexpressing BV2 cells with/out MK2206 treatment (N=3). G. Amount of IL-1β, IL-6 and TNF-α released into the supernatants of differentially-treated BV2 cells (N=3). H. Secreted LDH levels in the different groups (N=3). I-J. Pyroptosis-related proteins in the differentially-treated BV2 cells (N=3). *p < 0.05, **p < 0.01, ***p < 0.001 versus control; #p < 0.05, ##p < 0.01, ###p < 0.001 versus pc-CD73. K. Representative IHC images showing in situ expression of GSDMD and CASP-1 on the third day after SCI or sham surgery. L. BBB scores at different time points after SCI with/out SC79 treatment (N=6). *p < 0.05, **p < 0.01. Data are the mean ± SD from 3 independent experiments.

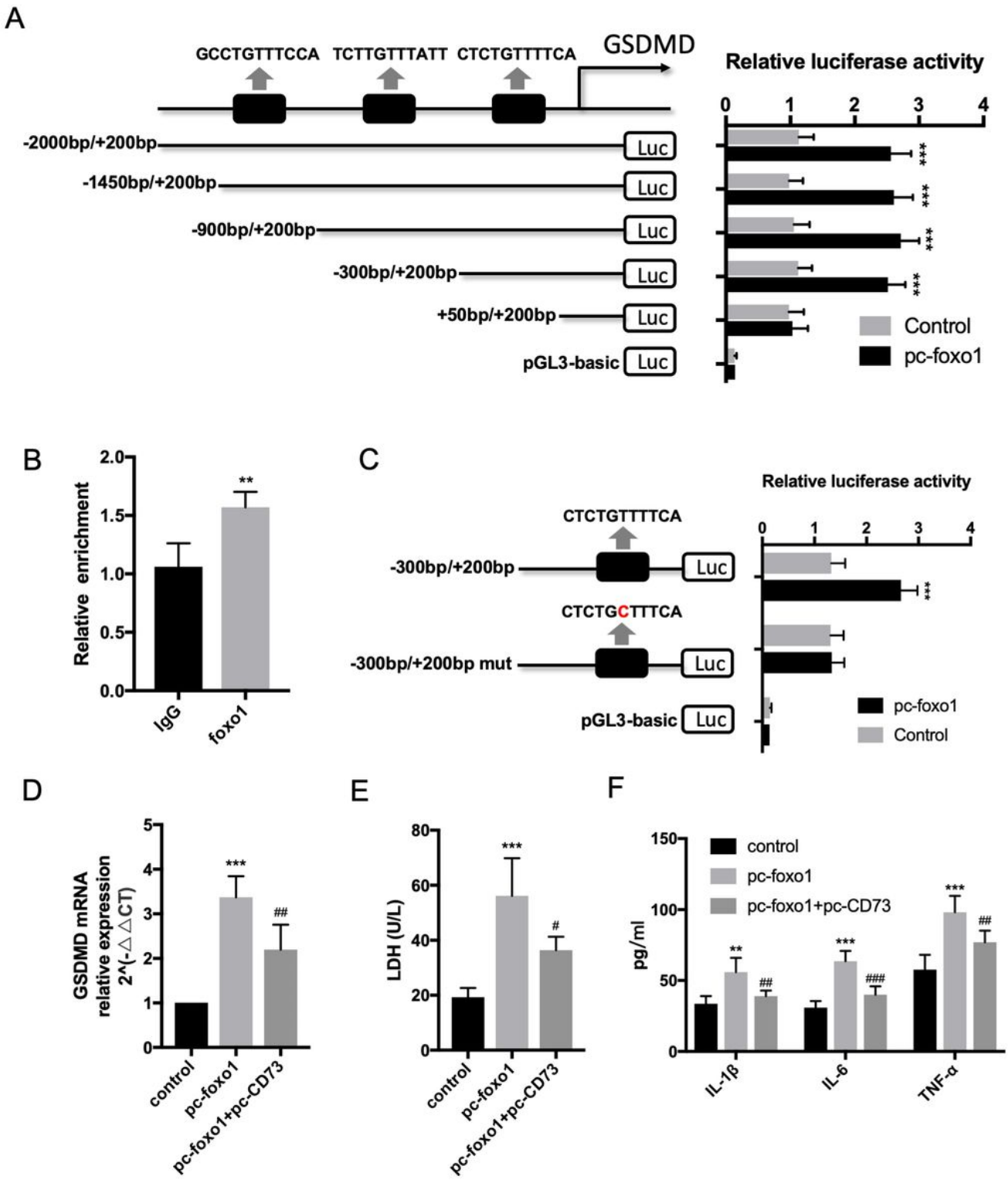

Figure 5

Foxo1 is a transcriptional activator of GSDMD. A. Luciferase activity of truncated GSDMD promoter-driven reporter gene (N=3). B. ChIP assay showing binding between GSDMD and FOXO1 (N=3). C. Luciferase activity of mutant GSDMD promoter-driven reporter gene. Mutated bases are shown in red (N=3). D. GSDMD mRNA levels in BV2 cells co-transfected with pc-Foxo1 and pc-CD73/empty vector (N=3). E. Secreted LDH levels in the different groups (N=3). F. IL-1β, IL-6 and TNF-α levels in the different

groups (N=3). **p < 0.01, ***p < 0.001 versus control; #p < 0.05, ##p < 0.01, ###p < 0.001 versus pc-Foxo1. Data are the mean ± SD from 3 independent experiments.

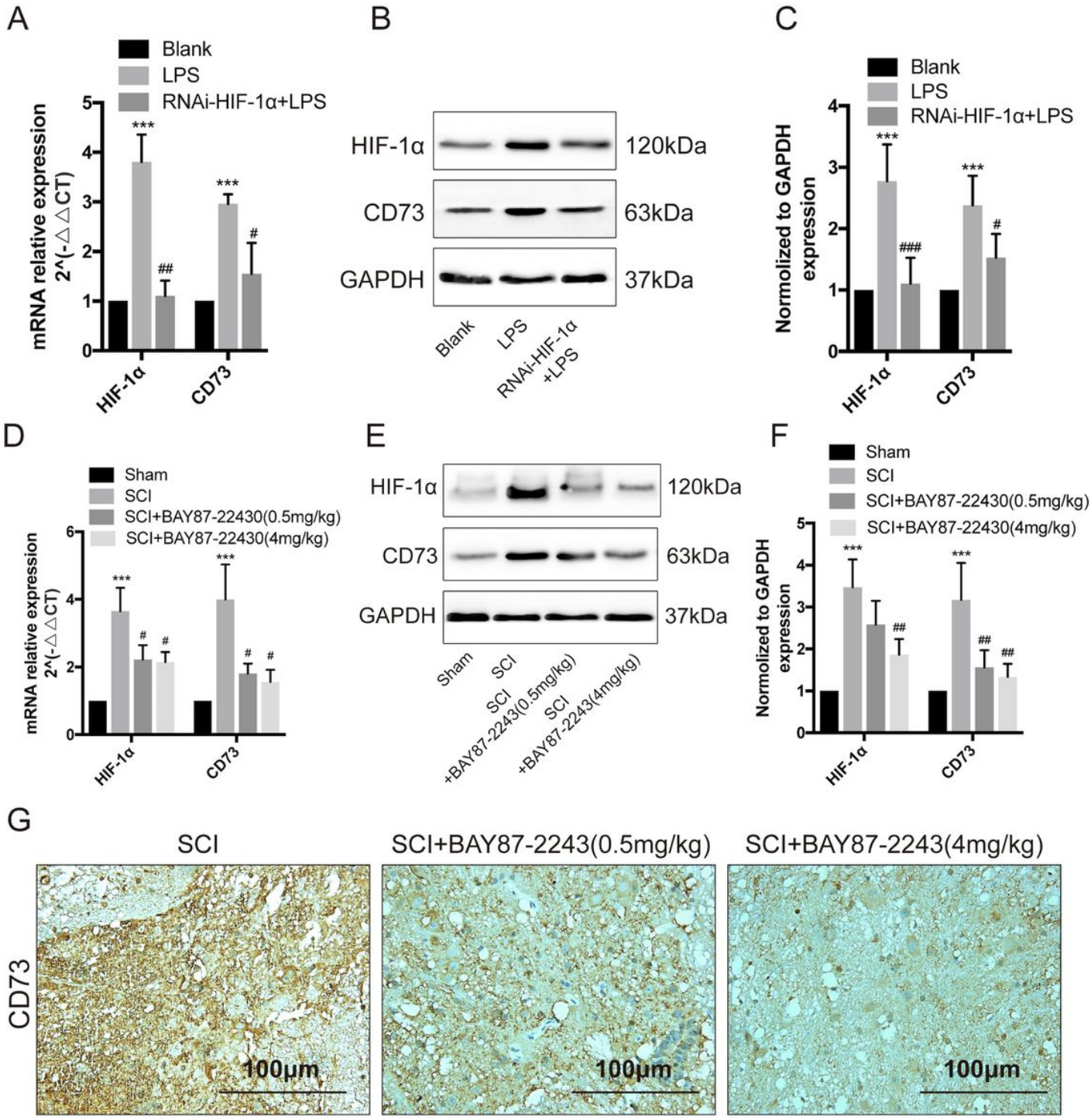

Figure 6

HIF-1α upregulates CD73 in microglia. A. HIF-1α and CD73 mRNA levels in BV2 cells challenged with LPS in the presence or absence of RNAi-HIF-1α (N=3). B-C. HIF-1α and CD73 protein levels in the above treated BV2 cells (N=3). D. HIF-1α and CD73 mRNA levels in WT mice 3 days post SCI with/out BAY87-22430 treatment (N=3). E-F. HIF-1α and CD73 protein levels in the above mice (N=3). G. Representative IHC

images showing in situ expression of CD73 in the spinal tissues of the above mice (N=3). ***p < 0.001 versus blank; #p < 0.05, ##p < 0.01, ###p < 0.001 versus LPS group. Data are the mean ± SD from 3 independent experiments.

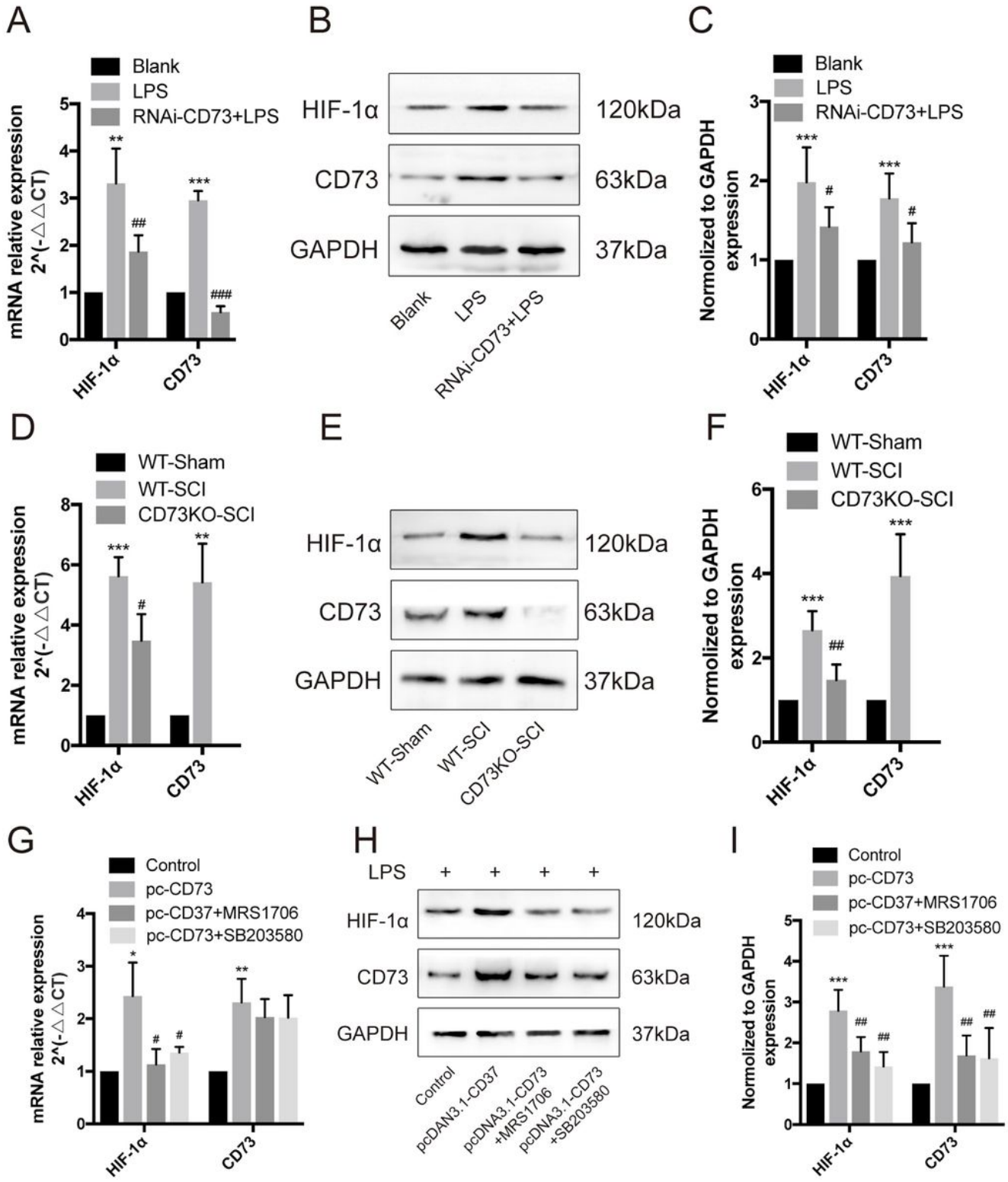

Figure 7

CD73 mediates HIF-1α accumulation in microglia. A. HIF-1α and CD73 mRNA levels in BV2 cells challenged with LPS in with/out RNAi-CD73 (N=3). **p < 0.01, ***p < 0.001 versus blank; ##p < 0.01,

###p < 0.001 versus LPS group. B-C. HIF-1α and CD73 protein levels in the above cells (N=3). ***p < 0.001 versus blank; #p < 0.05 versus LPS group. D. HIF-1α and CD73 mRNA levels in WT or CD73-KO mice 3 days post SCI (N=3). **p < 0.01, ***p < 0.001 versus WT-Sham; #p < 0.05 versus WT-SCI. E-F. HIF-1α and CD73 protein levels in the above mice (N=3). ***p < 0.001 versus WT-Sham; ##p < 0.01 versus WT-SCI. G. HIF-1α and CD73 levels in CD73-overexpressing BV2 cells challenged with LPS and MRS1706 (1μM) or SB203580 (10μM) (N=3). *p < 0.05, **p < 0.01 versus control; #p < 0.05 versus pc-CD73. H-I. HIF-1α and CD73 protein levels in the differentially-treated BV2 cells (N=3). ***p < 0.001 versus control; ##p < 0.01 versus pc-CD73. Data are shown as the mean ± SD from 3 independent experiments.

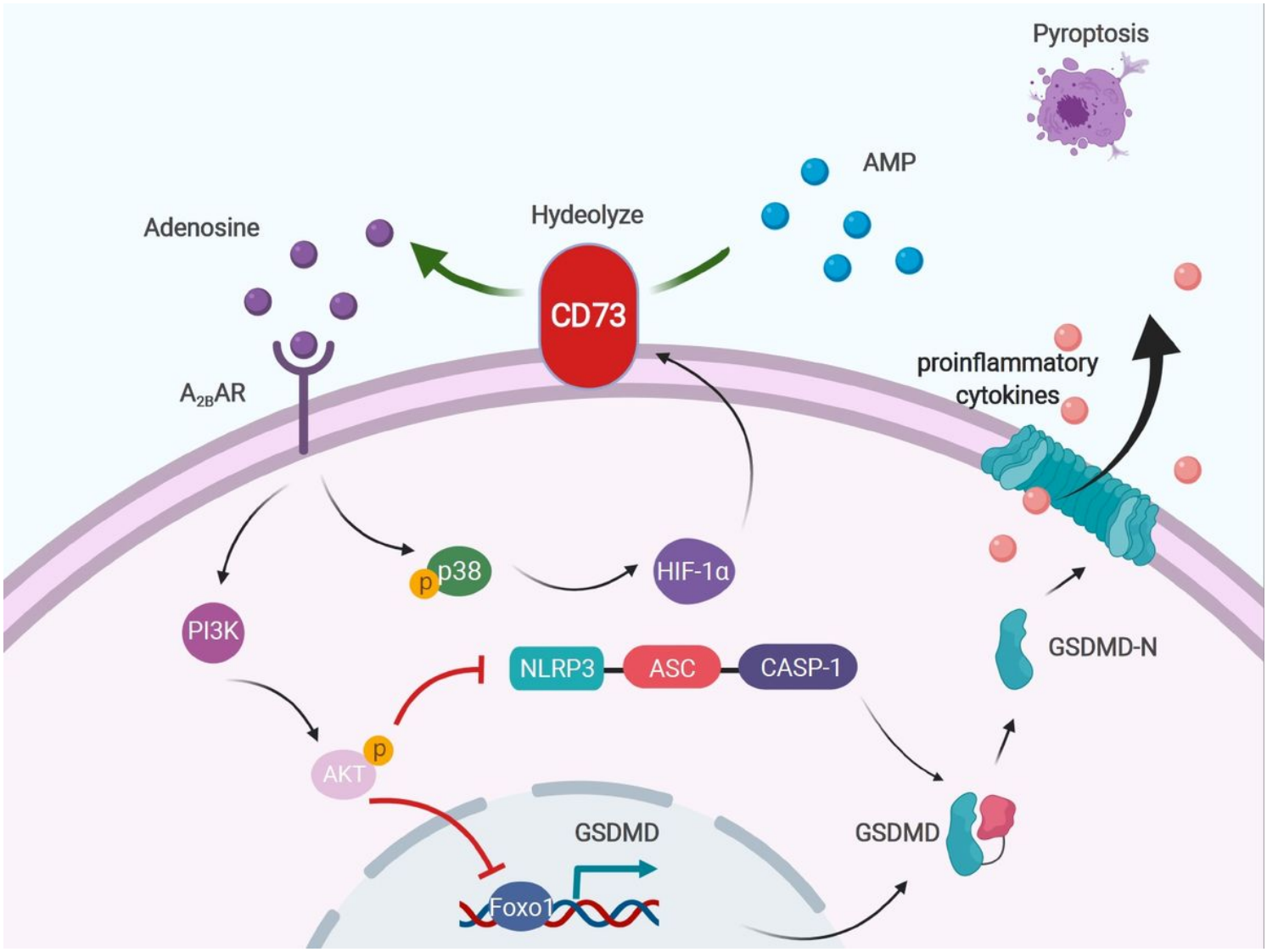

Figure 8

CD73 alleviates GSDMD-mediated pyroptosis by inhibiting PI3K/AKT/Foxo1 signaling. CD73 increases extracellular adenosine levels after injury, which activates the PI3K/AKT pathway via A2BAR, resulting in suppression of the NLRP3 inflammasome and GSDMD. The accumulation of HIF-1α after SCI upregulates CD73, which further increases HIF-1α levels through the adenosine-A2BAR-p38 cascade, thus forming a positive feedback regulation. This image is drawn with BioRender (www.biorender.com).

Supplementary Files

This is a list of supplementary files associated with this preprint. Click to download.

- S101.tif